

Numerical Study on the Impacts of Heterogeneous Reactions on Ozone Formation in the Beijing Urban Area

XU Jun^{*1,2} (徐 峻), ZHANG Yuanhang¹ (张远航), and WANG Wei² (王 玮)

¹ *College of Environmental Sciences, Peking University, Beijing 100871*

² *Chinese Research Academy of Environmental Sciences, Beijing 100012*

(Received 27 September 2005; revised 30 December 2005)

ABSTRACT

The air quality model CMAQ-MADRID (Community Multiscale Air Quality-Model of Aerosol Dynamics, Reaction, Ionization and Dissolution) was employed to simulate summer O₃ formation in Beijing China, in order to explore the impacts of four heterogeneous reactions on O₃ formation in an urban area. The results showed that the impacts were obvious and exhibited the characteristics of a typical response of a VOC-limited regime in the urban area. For the four heterogeneous reactions considered, the NO₂ and HO₂ heterogeneous reactions have the most severe impacts on O₃ formation. During the O₃ formation period, the NO₂ heterogeneous reaction increased new radical creation by 30%, raising the atmospheric activity as more NO→NO₂ conversion occurred, thus causing the O₃ to rise. The increase of O₃ peak concentration reached a maximum value of 67 ppb in the urban area. In the morning hours, high NO titration reduced the effect of the photolysis of HONO, which was produced heterogeneously at night in the surface layer. The NO₂ heterogeneous reaction in the daytime is likely one of the major reasons causing the O₃ increase in the Beijing urban area. The HO₂ heterogeneous reaction accelerated radical termination, resulting in a decrease of the radical concentration by 44% at the most. O₃ peak concentration decreased by a maximum amount of 24 ppb in the urban area. The simulation results were improved when the heterogeneous reactions were included, with the O₃ and HONO model results close to the observations.

Key words: heterogeneous reactions, ozone, air quality model, impacts, urban area

doi: 10.1007/s00376-006-0605-1

1. Introduction

Heterogeneous and multiphase reactions on solids and in liquids may have the potential to play a major role in determining the composition of the gaseous troposphere (Ravishankara, 1997). Heterogeneous reactions could affect O₃ concentrations in a number of ways including production and loss of HO_x (OH, HO₂, etc.) and NO_x, and direct loss of O₃, etc. (Jacob, 2000). As the features of air pollution are changing from typical coal-combustion pollution to a compound pollution case, O₃ and fine particles have become the major problem of urban or regional air pollution in China (Zhang et al., 1998). During an intensive monitoring campaign in summer 2000 in Beijing, high O₃ concentration, accompanied with high PM₁₀ concentration, appeared in both urban and suburban areas. Aerosols with high concentration levels supply a large surface area for heterogeneous reactions, which may

play an important role in the photochemical system of O₃ formation.

Some numerical simulation works have endeavored to identify the impacts of possible heterogeneous processes on dust or other aerosols, for species like NO₂, N₂O₅, HO₂, and O₃ etc., on O₃ formation. O₃ heterogeneous loss on dust could lead to a remarkable O₃ decrease in the dusty region, which has been testified by global 3-dimensional (3D) model simulations (Dentener et al., 1996), and an East Asian simulation by STEM-2K1 (Sulfur Transport Eulerian Model, version 2K1; Tang et al., 2003). Wang et al. (2000) designed a deflation module for use in modeling long-range transport of yellow sand over East Asia, establishing a platform for a further study of heterogeneous reactions on dust in the region. O₃ decrease made by the HO₂ heterogeneous reaction was small for global (Dentener et al., 1996) or regional scale (Horowitz et al., 1998) simulations. The impacts of the N₂O₅ heterogeneous re-

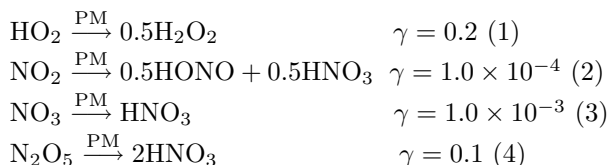
*E-mail: xujun@craes.org.cn

action on O_3 was also small in global scale (Dentener et al., 1996), European scale and southwestern Germany (Riemer et al., 2003) simulations. STEM-2K1 included an NO_2 heterogeneous loss on dust, but the reaction is an irreversible reaction with no recycling of NO_x , i.e., it did not produce gas phase HONO. In a Los Angeles 3D simulation by UAM (Calvert et al., 1994), O_3 increased by a maximum value of about 10 ppb by adding a new $NO_2 \rightarrow HONO$ heterogeneous conversion mechanism. Actually, there have not been many simulation works that have explored the effects of these heterogeneous reactions on polluted urban conditions. It is therefore meaningful to scrutinize the effects and the manner of action of each heterogeneous reaction on O_3 formation there.

With the fast urbanization in China, on top of the concentrated anthropogenic emission and fugitive dust effect, PM_{10} has become the prominent everyday pollutant for almost all of the major Chinese cities (see the daily air quality report: www.sepa.gov.cn/english/air-list.php3). The photochemical system under high aerosol concentration level could represent the characteristics of urban air pollution in China, and thus it deserves to be thoroughly studied. Here, we first explore the effect of the heterogeneous reactions possibly taking place on aerosol surfaces by means of a 3-D model simulation, with an emphasis on the impacts on O_3 formation in summer in the Beijing urban area.

2. Simulation description

CMAQ-MADRID (Zhang et al., 2004) was employed for the simulation. CMAQ-MADRID uses CMAQ (Byun and Ching, 1999) as a host model and improves all modules related to aerosol processes. Most aerosol dynamic processes were simulated, including new particle formation, growth by condensation, shrinkage by volatilization and gas/particle transfer. The particle size distribution is represented by a sectional approach with a user-selected option: 2 sections or 8 sections. In our simulation, the two-section size representation, typically for fine and coarse particles, was selected to reduce the computation time. In CMAQ-MADRID, no modifications were made to the transport modules of CMAQ, such as advection or turbulent diffusion. ISORROPIA (Nenes et al., 1998) was used as the thermodynamic module for gas-particle partition. CBIV (Carbon Bond mechanism, version IV; Gery et al., 1989) was selected as the gaseous chemical mechanism, and it included the four heterogeneous reactions suggested by Jacob (Jacob, 2000):



As a parameterization of the heterogeneous loss process, the first-order rate constant is calculated following Jacob, which is based on the radius of particles, the gas-phase molecular diffusion coefficient, mean molecular speed, reaction probability and the surface area of particles. The reaction probabilities, γ , used in our simulation were taken from the values proposed by Jacob, as shown in reactions (1)–(4), which were the base values of reaction probability on moist aerosol measured in the laboratory. As the relative humidity is high in summer in Beijing, it is appropriate to use the heterogeneous process parameter of moist aerosol for the simulation. The low solubility in water of O_3 precludes the significant uptake by moist aerosol (Jacob, 2000), and summertime in Beijing is not a dusty season, so, the effect of O_3 removal on dust or moist aerosol was not investigated here.

A three-level nesting was used for the simulation. The domain for the first level covered the whole of East Asia. The second level domain covered southern North China, including Hebei, Beijing, and Tianjin, and parts of the areas of Shanxi, Shandong, Liaoning and Inner Mongolia. The third level domain focused on the Beijing area, as shown in Fig. 1, including both urban and suburban areas of Beijing, with a horizontal resolution of 4 km. Fourteen layers were unequally spaced from the ground to roughly 10 km altitude, with 9 layers located under 1 km to resolve the boundary layer process. The simulation period was from 24 to 28 June 2000. The impacts of the four heterogeneous reactions mentioned above on O_3 formation were studied with a focus on the urban area. The Beijing urban area was confined to the area within the 4th ring road, and expanded slightly in all directions, having an area of 20 km \times 20 km, as shown in Fig. 1.

The meteorology field was derived from an MM5 [The Fifth-Generation PSU/NCAR (Pennsylvania State University/National Center of Atmospheric Research) Mesoscale Model, Grell et al., 1994] simulation. A 4-dimensional assimilation was made, using rawinsonde data and hourly data from ground stations in the urban and suburban areas of Beijing, to nudge the simulated meteorology variables close to the observations.

Both the emission factor method and the source survey were used for emission estimation in the Beijing area. The species included NO_x , VOCs, CO, SO_2 ,



Fig. 1. Model domain for the Beijing simulation and monitoring sites in the urban area (exterior frame delimits the 3rd level nested domain (144 km×144 km); interior frame delimits the urban area for the impact study).

PM₁₀ and NH₃. The basic data used for the emission estimation are: annual emission data and emission factors for a variety of sources reported by the local Environment Protection Bureau (EPB), statistical data of the environment, society and economy in North China, and a vegetation survey, etc. (Wang, 2002; Wang and Li, 2003). The VOC inventory in the Beijing area was compiled by sectors, such as, mobile sources, transportation and marketing of petroleum products, solvent utilization, industrial processes, and stationary source combustion, etc. Since there was not much detailed VOC speciation information measured for emission sources in China, the VOC speciation profile for each source type was defined by taking a reference from the United States Environmental Protection Agency (USEPA) method.

The 1°×1° anthropogenic emission inventory (Streets et al., 2003) maintained by CGRER (Center for Global and Regional Environmental Research) at the University of Iowa was used for the East Asia simulation (1st level domain), and the biogenic VOC emission was obtained from the GEIA (Global Emissions Inventory Activity) monthly global inventory (Guenther et al., 1995). SMOKE (Sparse Matrix Operator Kernel Emissions Sys-

tem: www.cmascenter.org/html/models.html) converted the various kinds of emission data to files with the format required by CMAQ.

3. Results

3.1 Aerosol simulation

Since PM₁₀ emission sources have highly random behavior, such as fugitive dust, it is almost impossible to make an accurate estimation for the PM₁₀ inventory. As shown in Fig. 2, during the simulation period, the observed hourly PM₁₀ mass concentration reached as high as 272 $\mu\text{g m}^{-3}$, with an average of 119 $\mu\text{g m}^{-3}$, which was at the typical PM₁₀ mass concentration level in summer in the Beijing urban area (Yu et al., 2005), and the simulated PM₁₀ mass concentration was at the same level of the observations. Although their hourly variations were not exactly matched, the simulated PM₁₀ level can represent the real situation in the Beijing urban area.

The observed concentration of aerosol surface area was not available for the simulation period. In 2004, the TDMPS (Twin Differential Mobility Particle Sizer) and APS (Aerodynamic Particle Sizer, TSI model 3321) systems were installed at Peking Univer-

sity to do aerosol sampling from March to August. They gave the range of aerosol surface area concentration from $227 \mu\text{m}^2 \text{cm}^{-3}$ on clear days to $3800 \mu\text{m}^2 \text{cm}^{-3}$ on smoky days (Hu Min, personal communication). As shown in Fig. 2, our simulation result was just in this range, which means that the real aerosol surface area concentration was well captured by our simulation. The sensitivity tests based on such an aerosol concentration level should be meaningful to explore the effects of heterogeneous reactions.

3.2 Impacts of heterogeneous reactions on O_3

From 26 to 27 June 2000, there was an occurrence of high O_3 concentration in the Beijing area. Some monitoring sites in the urban area recorded daily O_3 maximums exceeding 150 ppb. Relative humidity was also high for the two days. The aerosol surface area expands after absorbing water, which facilitates the heterogeneous reactions. Therefore, the two days were selected to scrutinize the impacts of heterogeneous re-

actions on O_3 formation, and a series of test runs was performed to detect the effect of each heterogeneous reaction on O_3 formation:

Control run—no heterogeneous reactions included,

NO_2 test run—only NO_2 heterogeneous reaction included,

$\text{NO}_2 + \text{NO}_3 + \text{N}_2\text{O}_5$ test run— NO_2 , NO_3 and N_2O_5 heterogeneous reactions included,

Full test run—all four (NO_2 , NO_3 , N_2O_5 and HO_2) heterogeneous reactions included.

Figure 3 gives the observed and simulated O_3 comparison averaged for the urban area. Generally, the simulated O_3 peak value and variation pattern match well with that of the observations, and the heterogeneous reactions do not alter the major characteristics of the O_3 variation pattern, yet the effects of the heterogeneous reactions are obvious. The response to the heterogeneous reactions exhibits the characteristics of a typical response of a VOC-limited regime for the Beijing urban area. The NO_2 heterogeneous reaction

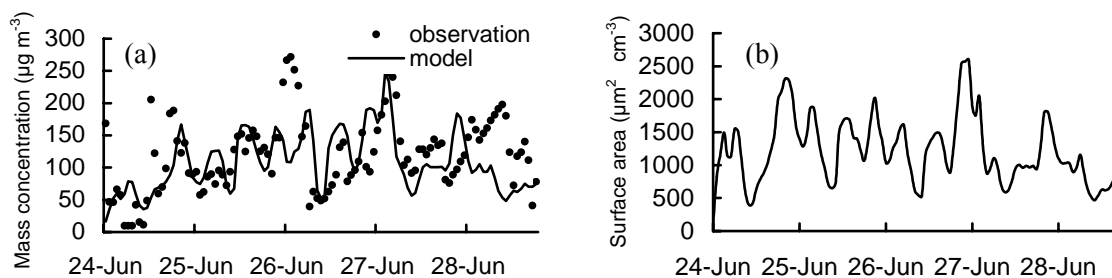


Fig. 2. PM_{10} simulation at ground level: (a) simulated and observed hourly PM_{10} mass concentration averaged over the urban area; (b) simulated hourly aerosol surface area concentration at Peking University.

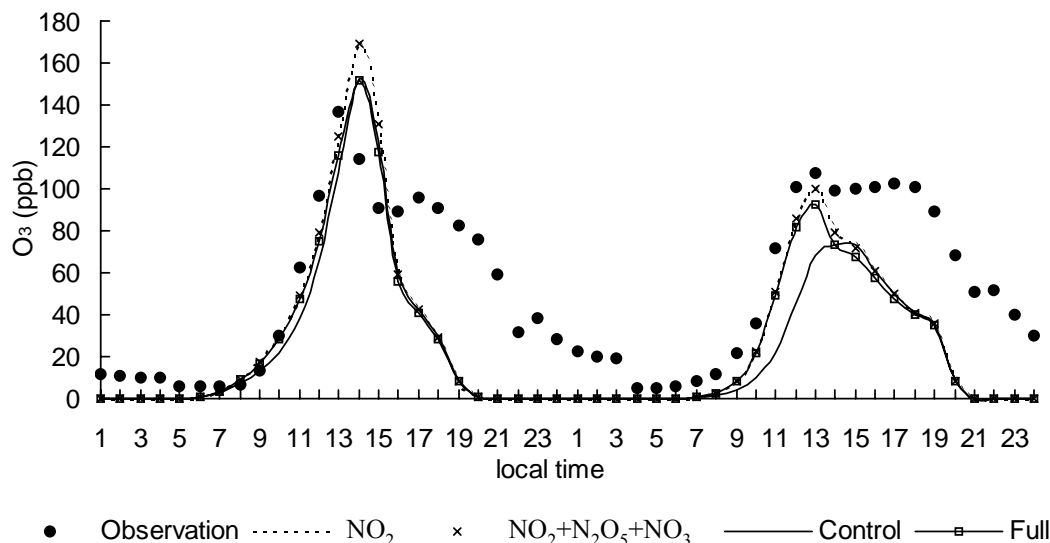


Fig. 3. Observed and simulated O_3 comparison with four test runs averaged over the urban area at the ground level from 26 to 27 June.

caused the O_3 to increase, especially for the O_3 ascending period, i.e., from the morning to the O_3 peak hour. When the NO_3 and N_2O_5 heterogeneous reactions were added ($NO_2+NO_3+N_2O_5$ test run), the O_3 concentration almost remains unchanged, indicating that the impacts of the NO_3 and N_2O_5 heterogeneous reactions on O_3 formation are quite small. The HO_2 heterogeneous reaction eliminated the radicals directly, leading to O_3 decrease, as in the Full test run. But, the O_3 decrease occurs mostly around the peak hour, since the radical concentration is the highest during that period of the day, causing a high efficiency of radical removal. The maximum impacts on O_3 concentration from the NO_2 and HO_2 heterogeneous reactions both appear around the O_3 peak hour. After including all four heterogeneous reactions, the O_3 increased during the O_3 ascending period and the simulated O_3 concentration was close to the observations at that time.

As shown in Fig. 4, the O_3 changes caused by both the NO_2 and HO_2 heterogeneous reactions mainly appear in the downwind area of the urban center, i.e., in the north, as a south wind prevailed during the two days. On 26 June, all of the maximum impacts from each heterogeneous reaction occurred at the Olympic Center (North 4th ring road), where the NO_2 heterogeneous reaction increased the O_3 by 37 ppb during the peak hour and the HO_2 heterogeneous reaction decreased the O_3 by 24 ppb. When all four heterogeneous reactions were included, the O_3 peak concentration increased by 15 ppb there. On 27 June, the distribution pattern of O_3 changes differed from that of 26 June, which was caused by a shift in wind direction. The maximum impacts on O_3 appeared further downwind in Qinghe, which is located in the northwest of the Beijing urban area. In the urban area, the maximum O_3 change occurred near Peking University (Northwest Beijing), where the NO_2 heterogeneous reaction caused the O_3 peak to increase by 67 ppb and the HO_2 heterogeneous reaction caused the O_3 peak to decrease by 17 ppb. Taking the four heterogeneous reactions altogether, the O_3 peak concentration increased by 50 ppb at Peking University.

So far, only few research studies have been designed to detect the effects of heterogeneous reactions on O_3 formation. In a Los Angeles 3D simulation (urban case) by UAM (Urban Airshed Model) (Calvert et al., 1994), O_3 increased by a maximum of about 10 ppb during 1100–1200 LST after adding a new HONO formation mechanism, i.e., the NO_2+H_2O reaction, specified in terms of gaseous species only. The O_3 increase was lower than that caused by the NO_2 heterogeneous reaction in our work. The discrepancy may be caused by the differences in the parameterizations of NO_2 to

HONO conversion and the emission characteristics of the two areas.

For the global (Dentener et al., 1996) or regional scale (Horowitz et al., 1998) simulations, the impacts of the HO_2 heterogeneous reaction on O_3 concentration were not as obvious as that in the Beijing urban area. In a 3D model simulation in summer over the southwestern part of Germany (Riemer et al., 2003), N_2O_5 heterogeneous hydrolysis decreased the O_3 concentration by a maximum amount of 5 ppb over the region, because almost all of the region belonged to the NO_x limited regime, which is opposite to the case of the Beijing urban area (illustrated in the next section).

Since the Olympic Center is located in the north part of the urban area, it belongs to the urban area and was in the downwind area of the urban center, where the photochemical reaction systems were well developed compared with that in the urban center. Therefore, the Olympic Center should be a good site to represent the characteristics of O_3 formation in the urban area. In the next section, a detailed analysis is made on the effects of the NO_2 and HO_2 heterogeneous reactions from the perspective of the chemical mechanism, to explore the process of the impacts on O_3 formation in an urban area.

3.3 NO_2 heterogeneous reaction

By analyzing the possible effects of the NO_2 heterogeneous reaction on O_3 formation through the view of the chemical mechanism, both products of the NO_2 heterogeneous reaction may lead to an O_3 increase in a radical-limited regime. The product, HONO, will create an OH radicals through photolysis, increasing the new radical creation. In a radical-limited regime, the atmospheric activity will rise, and more NO to NO_2 conversion will occur, leading to O_3 increase. The formation of another product, HNO_3 , is equivalent to eliminating NO_x directly from the systems. In a radical-limited regime, the OH radical, which should be terminated by the reaction $NO_2+OH\rightarrow HNO_3$, will continue in the radical cycles, thus the efficiency of the radical cycle rises and causes more $NO\rightarrow NO_2$ conversion. It is an indirect way to boost O_3 formation.

Process analysis measures, such as IPR (Integrated Process Rate analysis) and IRR (integrated reaction rate analysis) in CMAQ (Jeffries and Tonnesen, 1994), offer useful means to explore how the NO_2 heterogeneous reaction has an effect on O_3 formation. QSSA (Quasi-Steady State Approximation) was used as a gaseous chemistry solver, to ensure IRR tracking in each reaction of short life-time species. Next, a detailed analysis will be made with the radical pool (Bowman and Seinfeld, 1994) comparison and the evolution of changes leading to O_3 increase caused by the

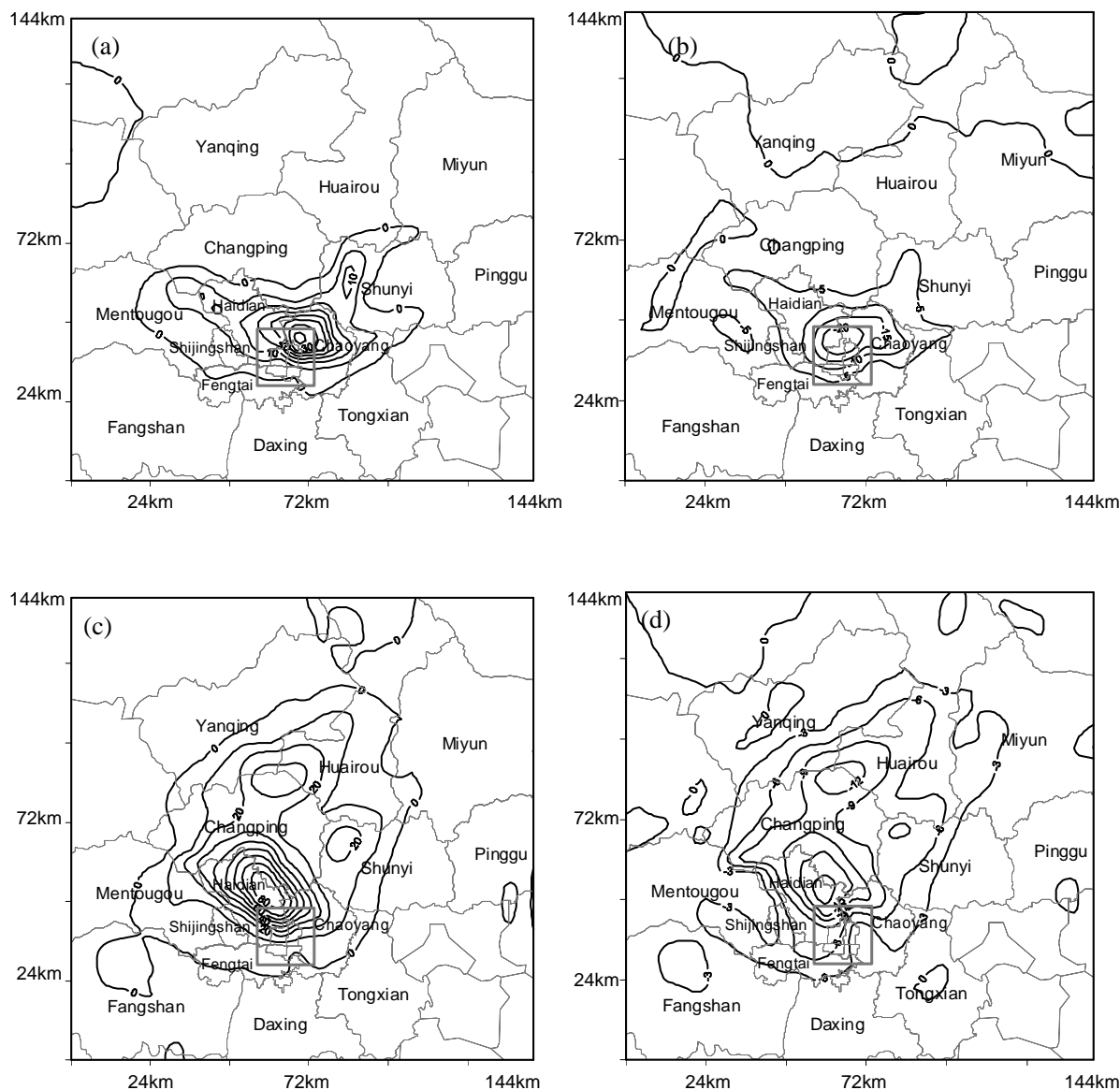


Fig. 4. Spatial distribution of O_3 difference made by each heterogeneous reaction at the O_3 peak hour at the ground level: (a) O_3 increase by the NO_2 heterogeneous reaction at 1400 LST 26 June (maximum: 36.7 ppb); (b) O_3 decrease by the HO_2 heterogeneous reaction at 1400 LST 26 June (maximum decrease: -24 ppb); (c) O_3 increase by the NO_2 heterogeneous reaction at 1200 LST 27 June (maximum: 89 ppb); (d) O_3 decrease by the HO_2 heterogeneous reaction at 1200 LST 27 June (maximum decrease: -18.9 ppb).

heterogeneous reaction.

3.3.1 Radical pool analysis

Radicals are the most active species in the atmospheric photochemical system, and the OH, RO_2 and HO_2 radicals play an important role in O_3 formation. Through photolysis of O_3 , aldehydes, HONO, and other species, new OH, RO_2 and HO_2 radicals are created and enter the radical cycle. The more new radicals created, the higher atmospheric activity it creates. In the cycle, the transfer between the RO_2 ,

HO_2 and OH radicals oxidizes VOC and converts NO to NO_2 , accomplishing the major oxidation processes in O_3 formation. Finally, they are eliminated by the termination paths of the RO_2 , HO_2 and OH radicals, respectively, due to the formation of HNO_3 , PAN, and H_2O_2 , etc. Such a radical pool, as shown in Fig. 5, can reveal the characteristics of new radical origin, the efficiency of the radical cycle, the atmospheric activity and the NO_x or VOC control regime of O_3 formation for specific locations. All items in the radical pool can be calculated through the IRR module in CMAQ. By

comparing the radical pools between cases with different selected heterogeneous reactions, the manner of effect of each heterogeneous reaction on O_3 formation could be further understood. Here, a typical period for O_3 formation, 0800–1600 LST 26 June, was selected to do the radical pool comparison.

As shown in Fig. 5, in the radical pool, although more than 2/3 of new radicals enter the radical cycle through the HO_2 and RO_2 path (for both cases), more than 80% of radicals were eliminated by the OH termination path, mainly through the reaction $NO_2 + OH \rightarrow HNO_3$. Sillman (1995) proposed a ratio, $P_{H_2O_2}/P_{HNO_3}$, to identify the NO_x or VOC regime for O_3 formation, where $P_{H_2O_2}$ and P_{HNO_3} are the production rates for H_2O_2 and HNO_3 respectively, with a transition ratio at 0.35. Since the major products of OH and HO_2 termination are HNO_3 and H_2O_2 respectively, $P_{H_2O_2}/P_{HNO_3}$ could be estimated by using the value of HO_2 and OH termination in the radical pool. For the two cases, the ratios were 0.01 and 0.03 respectively, which are both much lower than the transition ratio proposed by Sillman, indicating that radicals were scarce in the urban area and the case should be in a regime of VOC control (or called a radical-limited regime).

When the NO_2 heterogeneous reaction was included, new radical creation increased by 30%, i.e., 15 ppb, where 10 ppb came from an increase in new OH, and 4 ppb and 1 ppb came from increase in new HO_2 and RO_2 , respectively, as shown in Fig. 5. Within the 10 ppb increase of new OH radical, 7 ppb originated from HONO photolysis, which was the effect of the NO_2 heterogeneous reaction, and 2 ppb resulted from

the O_3 increase also by the effect of the NO_2 heterogeneous reaction. The increase of new RO_2 and HO_2 radical creation also resulted from an increase of new OH. As more new OH radical was created, more VOC could be oxidized by OH, with aldehyde as an intermediate product, which resulted in the increase in new HO_2 and RO_2 through aldehyde photolysis. It could be concluded that almost all of the increases of new radical creation was caused by HONO photolysis.

With the increase of new radical creation for the radical-limited regime, the atmosphere became more active. Each kind of radical transfer increased by about 30%, as shown in Fig. 5, indicating that more VOC was oxidized and more $NO \rightarrow NO_2$ conversion occurred. As more NO was converted to NO_2 by radicals, the NO_x cycle accelerated, leading to more O_3 formation.

In the Control run, a total of 199 ppb of radicals arrived at OH in the cycle, where 45 ppb of radicals were terminated by the OH termination path, mainly through the reaction $NO_2 + OH \rightarrow HNO_3$. The loss rate of OH radical by the termination path was 22.6%. After adding the NO_2 heterogeneous reaction, the loss rate of OH radical by the path became 20.7%, without much difference, indicating that the direct removal of NO_x (by forming the product HNO_3) in the NO_2 heterogeneous reaction only makes the loss rate of radicals by the path a little bit lower, and it cannot raise the efficiency of the radical cycles remarkably. It is HONO formed heterogeneously that made an increase of new radical creation, directly making up the scarcity of radicals in the urban area, accounting for the major reason of O_3 increase.

3.3.2 Process analysis

There is ample evidence that photolysis of HONO produced heterogeneously at night provides a major early-morning source of HO_x in high- NO_x environments (Harrison et al., 1996). As shown in Fig. 6, observed HONO at Peking University during the night reached 7–8 ppb, which is the typical HONO level in a high- NO_x area (Harris et al., 1982). Because of the fast photolysis in the daytime, HONO has a low concentration then. Without considering the NO_2 heterogeneous reaction, the simulated HONO has a very low concentration even for the nighttime (<1 ppb). When the NO_2 heterogeneous reaction is added, the HONO concentration increases remarkably during the night and reaches the observed level. In the Los Angeles simulation, HONO was also able to reach the observed level only after including the additional NO_2 to HONO conversion (Calvert et al., 1994). After sunrise, the photolysis of HONO accumulated at night is able to release the OH radical, raising the atmospheric

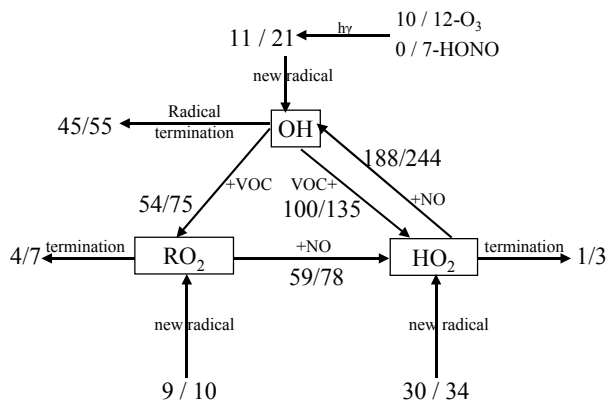


Fig. 5. Impact of the NO_2 heterogeneous reaction on the radical pool during 0800–1600 LST 26 June at the ground level of the Olympic Center (numbers by each arrow indicate the amount of radicals that follow each pathway over the duration of the simulation; each pair of numbers indicates the result from Control run and the result from the NO_2 test run, respectively; unit: ppb).

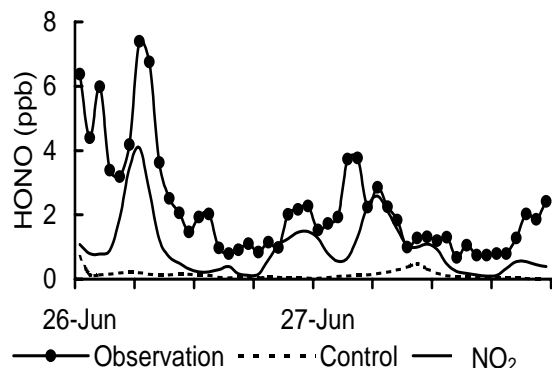


Fig. 6. Observed and simulated HONO comparison for cases with or without the NO_2 heterogeneous reaction included at the ground level of Peking University from 26 to 27 June.

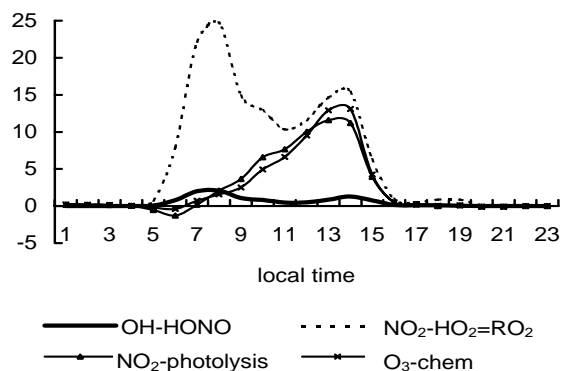


Fig. 7. NO_2 heterogeneous effects on relevant chemical processes for O_3 formation at the surface layer of the Olympic Center on 26 June (OH-HONO denotes the increase of new OH radical creation by HONO photolysis; O_3 -chem denotes the increase of O_3 production by the chemical process; NO_2 -photolysis denotes the increase of net production of NO_2 photolysis, which is the net production of reactions $\text{NO}_2 + h\nu \rightarrow \text{NO} + \text{O}_3$ and $\text{O}_3 + \text{NO} \rightarrow \text{NO}_2$; $\text{NO}_2\text{-HO}_2=\text{RO}_2$ denotes the increase of $\text{NO} \rightarrow \text{NO}_2$ conversion by the HO_2 and RO_2 radicals).

activity.

In the radical-limited regime, the photolysis of HONO produced heterogeneously may increase the $\text{NO} \rightarrow \text{NO}_2$ conversion and cause the O_3 to rise. Figure 7 gives the hourly changes made by the NO_2 heterogeneous reaction for the relevant chemical processes in one day, in order to check the evolution of the heterogeneous effects. In the surface layer, the increase of the $\text{NO} \rightarrow \text{NO}_2$ conversion had two peaks during the daytime, one occurring in the morning and the other in the O_3 peak period, corresponding to the two large increases of OH radical creation caused by the HONO photolysis. The high increase of radical creation in the morning was caused by the photolysis of HONO, which

was accumulated through the NO_2 heterogeneous reaction during the nighttime. During the O_3 peak period, the photochemistry was the most active, and the NO_2 produced chemically reached its aximum then, thus the NO_2 heterogeneous reaction could reach a high level of activity, leading to a large increase in radical creation for the period.

In the morning hours, because the boundary layer is not yet fully developed, NO_x concentration is much higher in the surface layer than in the upper level, and accumulated HONO was condensed at the lower level, leading to a large increase of $\text{NO} \rightarrow \text{NO}_2$ conversion in the surface layer. From the view of the chemistry mechanism of O_3 formation, a large increase in $\text{NO} \rightarrow \text{NO}_2$ conversion should lead to a corresponding large increase in O_3 production. But for the surface layer, the large increase in $\text{NO} \rightarrow \text{NO}_2$ conversion in the morning did not switch to a large increase of O_3 production then. Since the photochemistry was not very active in the morning hours, NO comprised a major part of NO_x in the surface layer. Although the increase of NO_2 photolysis was high during the period, most O_3 produced by NO_2 photolysis was consumed by NO titration, causing a slow increase in the net production of NO_2 photolysis, which led to a small increase of O_3 produced chemically.

As the atmospheric activity became more active with time, the percentage of NO_2 covered by NO_x grew, so, the net production of NO_2 photolysis rose gradually by way of the decrease of NO titration. At the O_3 peak hour, the photochemistry was the most active, with NO_2 comprising a major part of the NO_x in the surface layer, causing a low NO titration then, thus, most of the increase of $\text{NO} \rightarrow \text{NO}_2$ conversion could switch to the net production of NO_2 photolysis. Since the increase of $\text{NO} \rightarrow \text{NO}_2$ conversion reached a peak in the O_3 peak hour, it caused the highest O_3 production increase at that time.

In the morning hours, high NO titration reduced the effect of the photolysis of HONO, which was accumulated heterogeneously during the nighttime in the surface layer. The NO_2 heterogeneous reaction in the daytime should be one of the major reasons for the O_3 increase in the Beijing urban area.

3.4 HO_2 heterogeneous reaction

When the HO_2 heterogeneous reaction was added, radical termination was accelerated, resulting in a decrease of radical concentration. As shown in Fig. 8, all of the concentrations of OH, HO_2 and RO_2 decreased remarkably, with the same variation pattern. The HO_2 concentration decreased by the most severe factor, by a maximum amount of about 44%, which occurred at the O_3 peak hour.

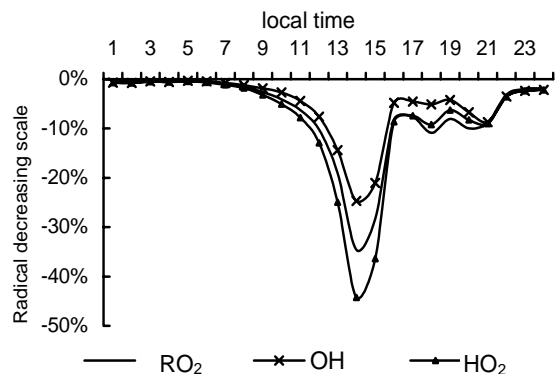


Fig. 8. Decreasing scale of radical concentration caused by the HO_2 heterogeneous reaction for 26 June at the ground level of the Olympic Center.

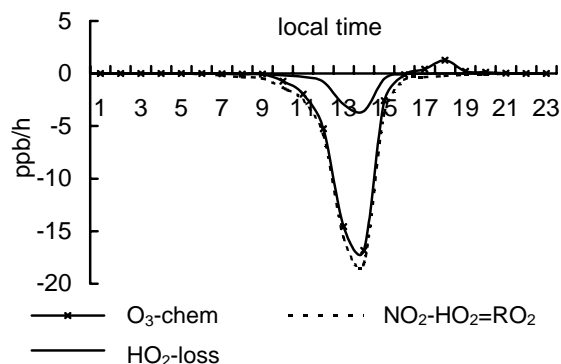


Fig. 9. HO_2 heterogeneous effects on relevant processes for O_3 formation in the surface layer on 26 June ($\text{O}_3\text{-chem}$ denotes the decrease of O_3 production by the chemical process, $\text{NO}_2\text{-HO}_2=\text{RO}_2$ denotes the decrease of $\text{NO}\rightarrow\text{NO}_2$ conversion by the HO_2 and RO_2 radicals, $\text{HO}_2\text{-loss}$ denotes the HO_2 radical loss by its heterogeneous reaction).

As some radicals were terminated by the extra path, the efficiency of the radical cycles declined, leading to a fall in atmospheric activity. During the O_3 peak period, the atmosphere was the most active, and radical concentration was also the highest then. As shown in Fig. 9, HO_2 heterogeneous loss was the most intensive for the period. Since the urban area was in a radical-limited regime, it brought a sharp decline in $\text{NO}\rightarrow\text{NO}_2$ conversion, and caused a remarkable decrease in O_3 production at that time.

4. Summary

The air quality model CMAQ-MADRID was employed to simulate summer O_3 and aerosol concentration in Beijing in order to explore the impacts of four heterogeneous reactions on O_3 formation in an urban area. The heterogeneous reactions were parameterized in a heterogeneous loss process of gaseous species on

aerosols, which was mainly based on the simulation of aerosol surface area and the reaction probability of gaseous species, etc. The results showed that the impacts were obvious and exhibited a typical response of a VOC-limited regime for an urban area. For the four heterogeneous reactions considered, the NO_2 and HO_2 heterogeneous reactions have the most severe impacts on O_3 formation. During the O_3 building period, the NO_2 heterogeneous reaction increased new radical creation, leading to an increase in $\text{NO}\rightarrow\text{NO}_2$ conversion, causing O_3 to rise in the Beijing urban area. The HO_2 heterogeneous reaction lowered the radical propagation efficiency, reducing the radical concentration, and causing the O_3 to decrease. The simulation results were improved when the heterogeneous reactions were included.

So far, only a few modeling studies have tested the effects of heterogeneous reactions, and only simplified heterogeneous reaction processes are used in air quality models. A better understanding of the heterogeneous mechanisms is highly desirable for the improvement of the models. More detailed consideration of the possible effects of surface saturation, as well as competition for reactions, need to be considered (Tang et al., 2003). Although some heterogeneous reaction mechanisms or the coefficients in the reactions need to be further confirmed in both experiments and field studies, it is essential to include them in the simulation of O_3 and aerosol components under such a high aerosol concentration level as is found in Chinese urban areas. In addition, UV-scattering or UV-absorbing aerosols may alter the actinic flux of UV, which could affect O_3 formation (Dickerson et al., 1997). Both radiative and heterogeneous reaction influences of aerosols may have effects on the photochemical system in the urban areas of China, therefore, related studies should be performed to quantify the role of each influence on the urban atmosphere.

Acknowledgments. This work was supported by the national 973 projects (2002CB410800) and Social Public Welfare Project from Ministry of Science and Technology of the People's Republic of China (MOST) (2002DIA20012, ABC project)

REFERENCES

- Bowman, F. M., and J. H. Seinfeld, 1994: Ozone productivity of atmospheric organics. *J. Geophys. Res.*, **99**, 5309–5324.
- Byun, D. W., and J. K. S. Ching, Eds., 1999: Science algorithms of the EPA Models-3 community multi-scale air quality (CMAQ) modeling system. Rep. EPA-600/R-99/030, National Exposure Research Laboratory, Research Triangle Park, N.C., Chapter 1, 18pp.

- Calvert, J. G., G. Yarwood, and A. M. Dunker, 1994: An evaluation of the mechanism of nitrous acid formation in the urban atmosphere. *Research on Chemical Intermediates*, **20**, 463–502.
- Dentener, F., G. R. Carmichael, Y. Zhang, J. Lelieveld, and P. J. Crutzen, 1996: Role of mineral aerosol as reactive surface in the global troposphere. *J. Geophys. Res.*, **101**(D17), 22869–22889.
- Dickerson, R. R., S. Kondragunta, G. Stenchikov, K. L. Civerolo, B. G. Doddridge, and B. N. Holben, 1997: The impacts of aerosols on solar ultraviolet radiation and photochemical smog. *Science*, **278**, 827–830.
- Gery, M. W., G. Z. Whitten, J. P. Killus, and M. C. Dodge, 1989: A photochemical kinetics mechanism for urban and regional scale computer modeling. *J. Geophys. Res.*, **94**, 12,925–12,956.
- Grell, G. A., J. Dudhia, and D. R. Stanffer, 1994: A description of the Fifth-generation Penn State/NCAR Mesoscale Model (MM5). NCAR Tech. Note, NCAR/TN-398 + STR, 138pp.
- Guenther, A., and Coauthors, 1995: A global model of natural volatile organic compound emissions. *J. Geophys. Res.*, **100**, 8873–8892.
- Harris, G. W., W. P. L. Carter, A. M. Winer, J. N. Pitts, U. Platt, and D. Perner, 1982: Observations of nitrous acid in the Los Angeles atmosphere and implications for the predictions of ozone-precursor relationships. *Environ. Sci. Technol.*, **16**, 414–419.
- Harrison, R. M., J. D. Peak, and G. M. Collins, 1996: Tropospheric cycle of nitrous acid. *J. Geophys. Res.*, **101**, 14429–14439.
- Horowitz, L. W., J. Liang, G. M. Gardner, and D. J. Jacob, 1998: Export of reactive nitrogen from North America during summertime: Sensitivity to hydrocarbon chemistry. *J. Geophys. Res.*, **103**(D11), 13451–13476.
- Jacob, D., 2000: Heterogeneous chemistry and tropospheric ozone. *Atmos. Environ.*, **34**, 2132–2159.
- Jeffries, H. E., and S. Tonnesen, 1994: A comparison of two photochemical reaction mechanisms using mass balance and process analysis. *Atmos. Environ.*, **28**(18), 2991–3003.
- Nenes, A., S. N. Pandis, and C. Pilinis, 1998: ISOR-ROPIA: A new thermodynamic model for inorganic multicomponent atmospheric aerosols. *Aquatic Geochemistry*, **4**, 123–152.
- Ravishankara, A. R., 1997: Heterogeneous and multiphase chemistry in the troposphere. *Science*, **276**, 1058–1065.
- Riemer, N., H. Vogel, B. Vogel, B. Schell, I. Ackermann, C. Kessler, and H. Hass, 2003: Impact of the heterogeneous hydrolysis of N_2O_5 on chemistry and nitrate aerosol formation in the lower troposphere under photochemical conditions. *J. Geophys. Res.*, **108**(D4), 4144, doi: 10.1029/2002JD002436.
- Sillman, S., 1995: The use of NO_y , H_2O_2 , and HNO_3 as indicators for ozone- NO_x -hydrocarbon sensitivity in urban locations. *J. Geophys. Res.*, **100**(D7), 14175–14188.
- Streets, D. G., and Coauthors, 2003: An inventory of gaseous and primary aerosol emissions in Asia in the year 2000. *J. Geophys. Res.*, **108**(D21), 8809, doi: 10.1029/2002JD003093.
- Tang, Y., and Coauthors, 2003: The impacts of dust on regional tropospheric chemistry during the ACE-ASIA experiment: A model study with observations. *J. Geophys. Res.*, **108**(D21), doi: 10.1029/2003JD003506.
- Wang, Z., H. Ueda, and M. Huang, 2000: A deflation module for use in modeling long-range transport of yellow sand over East Asia. *J. Geophys. Res.*, **105**(D22), 26947–26959.
- Wang Xuesong, 2002: A numerical simulation study on ozone and secondary aerosol in Regional atmosphere. Ph.D dissertation, College of Environmental Sciences, Peking University, Beijing. (in Chinese)
- Wang Xuesong, and Li Jinlong, 2003: A case study of ozone source apportionment in Beijing. *Acta Scientiarum Naturalium Universitatis Pekinensis*, **39**(2), 244–253. (in Chinese)
- Yu Jiahua, G. Benjamin, Yu Tong, Wang Xin, and Liu Wenqing, 2005: Seasonal variations of number size distributions and mass concentrations of atmospheric particles in Beijing. *Adv. Atmos. Sci.*, **22**(3), 401–407.
- Zhang, Y., and Coauthors, 2004: Development and application of the Model of Aerosol Dynamics, Reaction, Ionization and Dissolution (MADRID). *J. Geophys. Res.*, **109**, D01202, doi: 10.1029/2003JD003501.
- Zhang Yuanhang, Shao Kesheng, Tang Xiaoyan and Li Jinlong, 1998: The study of urban photochemical smog pollution in China. *Acta Scientiarum Naturalium Universitatis Pekinensis*, **34**(2–1), 392–400. (in Chinese)